ELSEVIER

Catalysis Today 71 (2001) 3–10

CATALYSIS TODAY

www.elsevier.com/locate/cattod

A combined experimental and theoretical approach to the study of methane activation over oxide catalysts

Christopher A. Cooper [a], Charles R. Hammond [a], Graham J. Hutchings [a,*], Stuart H. Taylor [a], David J. Willock [a], Kenji Tabata [b]

[a] *Department of Chemistry, Cardiff University, P.O. Box 912, Cardiff CF10 3TB, UK*
[b] *RITE Foundation, 9-2 Kizugawadai, Kizu-Cho, Soraku-Gun, Kyoto 619-0292, Japan*

Abstract

We present new results on the activation of methane over pure and doped gallium oxide catalysts. This catalyst was selected from our earlier work on methane to methanol conversion over mixed oxide systems. Calculations show that for defect free surfaces of the β-Ga_2O_3 phase only the (0 1 0) and (0 0 1) facets are stable. Density functional theory level calculations are presented which show that the (0 1 0) surface undergoes only a small amount of re-construction from the bulk structure. This suggests that the real crystal surfaces will be defective and we have attempted to increase the surface concentration of defects further by doping with divalent cations. Zn doping leads to an increase in activity compared to β-Ga_2O_3, whilst Mg doping decreased the activity.

Keywords: Gallium oxide; Methane oxidation

1. Introduction

The selective activation of methane remains one of the biggest challenges facing scientists interested in the design of heterogeneous catalysts. In particular, the selective oxidation to yield C_2 hydrocarbon products (oxidative coupling) or methanol have been extensively studied since Lunsford and Ito [1] first indicated that the oxidative coupling reaction could be catalysed by Li doped MgO. Subsequently, many researchers [2,3] showed that most oxides and oxide combinations could be used to catalyse this reaction. Two observations became apparent. First, it was observed that the methane conversion and C_2 selectivity usually summed to 100%, known as the 100% rule. Second, C_2 hydrocarbon yields in excess of 30% were extremely rare [2].

Later, it became apparent that the bulk of the reactions occurring during the methane oxidative coupling reactions were homogeneous gas phase reactions. Methane was homolytically activated at a surface oxide site to form gas phase methyl radicals, which either dimerised to form hydrocarbons (1) or formed oxygenates and carbon oxides (2) [2,3]:

$$2CH_3^{\bullet} \rightarrow C_2H \overset{\Delta, H_2O}{\rightarrow} C_2H_4 \quad (1)$$

$$CH_3^{\bullet} + O_2 \rightarrow CH_2O/CH_3OH \rightarrow CO/CO_2 + H_2O \quad (2)$$

The control of the product distribution, i.e. whether hydrocarbons or oxygenates, was observed to be achieved through variation of the oxygen

* Corresponding author. Tel.: +44-29-2087-4805; fax: +44-29-2087-4075.
E-mail addresses: hutch@cf.ac.uk, reganp@cf.ac.uk (G.J. Hutchings).

0920-5861/01/$ – see front matter
PII: S0920-5861(01)00446-1

concentration [4]. At low oxygen concentrations, the dimerisation reaction was favoured. However, both the formation of hydrocarbon or oxygenate products involved the extensive involvement of gas phase radical reactions, which are predominant at the high reaction temperatures (>600°C) required for the activation of methane on oxide surfaces.

We have recently reconsidered the problems associated with the scientific design of catalysts for the selective activation of methane, and details of preliminary experiments to further probe the activation of methane in the context of designing improved methane partial oxidation catalysts are presented. One of the most important aspects of methane oxidation is activation, and it has been proposed that the role of defects are crucial for methane activation [2]. In this paper, we aim to investigate the activation of methane over gallium oxide and gallium oxide doped with magnesium and zinc in an attempt to increase the defect concentration.

2. Design approach for methane partial oxidation

There are several notable approaches to the design of effective methane partial oxidation catalysts in scientific literature. One of the earliest is described by Dowden et al. [5], who developed a catalyst formulated on the basis of a proposed virtual mechanism. Other approaches, such as those described by Otsuka and Hatano [6] and Lyons et al. [7], have also proved successful in creating new methane partial oxidation catalysts.

The design approach outlined in this study has been presented fully and discussed at length elsewhere [8,9] and is summarised in the following section. The approach is an attempt to combine components with the desired reactivity; it is considered that a successful methane partial oxidation catalyst must:

1. not destroy the desired product, methanol;
2. activate methane;
3. activate oxygen.

The majority of catalysts used for methane partial oxidation are metal oxides and we have investigated these processes over a wide range of single metal oxides in an attempt to combine the necessary functions in a single catalyst.

The activation of methanol was probed by studying methane oxidation over single oxides and the prime requisite is that a suitable catalyst component must not readily destroy methanol under reaction conditions. The activation of methane was investigated by studying the rate of CH_4/D_2 exchange. Oxygen activation was characterised by $^{16}O_2/^{18}O_2$ exchange. Thus, simplistically, it can be imagined that synergistic combinations may exist in which one component is principally responsible for methane activation and the other for oxygen activation/insertion. This type of approach is not without precedent, as one of the currently accepted views of the mode of operation of the bismuth molybdate catalyst for propene oxidation and ammoxidation is that the bismuth component is responsible for hydrocarbon activation, whilst the molybdenum component effects oxygen activation and insertion [10].

Studies to assess methanol stability show that it is most stable over the oxides MoO_3, WO_3, Nb_2O_5, Ta_2O_5 and Sb_2O_3. In particular, the conversion of methanol to carbon oxides over MoO_3 was very low, whilst showing high selectivity towards formaldehyde. Additionally, the oxygen exchange reaction over MoO_3 takes place with the entire bulk of the oxide. This suggests that the diffusion of oxygen through the lattice of these solids is faster than the surface exchange, which is, therefore, the rate determining process. This is an important concept for selective oxidation reactions in which labile lattice oxygen is the active oxygen species.

Methane/deuterium exchange studies show that Ga_2O_3 is significantly more active for the activation of methane compared with other catalysts by several orders of magnitude. ZnO also exhibited high activity for the exchange reaction and it is interesting to note that both the elements show high activity for alkane activation such as amortisation processes of short chain alkanes when in combination with MFI type zeolites [11].

Based on the results detailed above, a Ga_2O_3/MoO_3 catalyst was prepared and results for methane oxidation are shown in Table 1. The Ga_2O_3/MoO_3 catalyst produced the highest catalytic yield of methanol which was greater than the comparative homogeneous gas phase reaction over a quartz chips packed reactor. The methanol yields over MoO_3 and Ga_2O_3 were also low in comparison with Ga_2O_3/MoO_3. Methane oxidation over MoO_3 showed that the oxide was rela-

Table 1
Methane oxidation over Ga_2O_3/MoO_3 physical mixture[a]

Catalyst	Temperature (°C)	CH_4 conversion (%)	Selectivity (%)				CH_3OH per pass yield
			CH_3OH	CO	CO_2	C_2H_6	
Ga_2O_3/MoO_3	455	3.0	22	50	27	1	0.66
Ga_2O_3	455	1.5	3	27	68	2	0.05
MoO_3	455	0.3	13	69	18	–	0.04
Quartz packing	455	0.1	–	–	100	–	0.00
Empty tube	455	8.1	29	63	7	1	2.34

[a] $CH_4/O_2/He = 23/2/5$, 15 bar, GHSV = 5000 h^{-1}.

tively selective for methanol, whilst Ga_2O_3 was more active, showing a much higher methane conversion. These observations are consistent with the high activity for methane activation of Ga_2O_3, as discussed previously in relation to methane/deuterium exchange, as well as the oxygen exchange mechanism and the selective oxidation function exhibited by MoO_3 during methanol oxidation studies. These aspects were beneficially combined for methane partial oxidation by the physically mixed Ga_2O_3/MoO_3 system.

The results obtained clearly indicate that the design approach is valid and the concept has resulted in the manufacture of a novel catalyst system based on gallium and molybdenum oxides, which shows promising activity for the partial oxidation of methane to methanol. However, the yield of methanol from the empty reactor tube was considerably higher than from the Ga_2O_3/MoO_3 catalyst. This was primarily a consequence of the higher methane conversion and was not due to an increase in methanol selectivity. The increase in conversion can be explained in terms of increased residence time within the heated zone of the empty reactor compared with the reactor packed with catalyst.

The present study was started to investigate further the important steps in the partial oxidation reaction. The property of high efficacy for methane activation by Ga_2O_3 is the most significant result of these preliminary studies and is an elementary step in the partial oxidation process. The present communication details our initial results probing the relationship between Ga_2O_3 structure and chemistry and the ability to activate methane. These studies have used a combined experimental and theoretical approach and have aimed at investigating the effect of doping Ga_2O_3, with the ultimate aim of determining the role of defects on catalysis. Gallium oxide has been doped with zinc and magnesium as these components have also shown promising activity for methane activation [8]; additionally the ions are of comparable ionic radius to Ga^{3+} and their incorporation in the lattice will increase the defect concentration.

3. Experimental

3.1. Catalyst preparation

A series of gallium oxide based catalyst was prepared. Ga_2O_3 was prepared by dissolving gallium nitrate in deionised water. The solution was thoroughly stirred for 30 min and dilute ammonia solution was added dropwise until pH 8.5 was attained. The gelatinous precipitate was stirred in the liquor for a further 30 min and then collected by filtration. The resultant gel was calcined in air, using a temperature-programmed regime from ambient to 700°C at 20°C min^{-1}, and then maintained at 700°C for 14 h. The zinc doped Ga_2O_3 (Zn:Ga = 1:99 wt.%) was obtained by a coprecipitation method. A mixed solution of gallium and zinc was prepared by dissolving appropriate quantities of the respective nitrates in deionised water. The resulting solution was thoroughly stirred for 30 min and dilute ammonia solution was added dropwise until pH 8.5 was attained. The gelatinous precipitate was stirred in the liquor for a further 30 min and then collected by filtration. The precipitate was calcined using the same procedure adopted for Ga_2O_3 preparation.

It was not possible to prepare a magnesium doped gallium oxide catalyst (Mg:Ga = 1:99 wt.%) using the same coprecipitation method. The variation in

preparation method was adopted as gallium and magnesium nitrates precipitate at vastly different pH resulting in a catalyst with poor homogeneity. For comparison, a coprecipitated magnesium/gallium catalyst was prepared from magnesium phosphate and gallium nitrate as they precipitate at similar pH. The coprecipitated magnesium phosphate doped Ga_2O_3 (Mg:Ga = 1:99 wt.%) was prepared from a mixed solution of the salts by dissolving appropriate quantities of the chemicals in deionised water. The resulting solution was stirred for 30 min and dilute ammonia solution was added dropwise until a pH of 8 was attained. The gelatinous precipitate was then stirred for a further 30 min and then collected by filtration. The precipitant was again calcined using the same procedure as in the preparation of the Ga_2O_3. For comparison, zinc oxide and magnesium phosphate catalysts were prepared by precipitation methods. The zinc oxide system was precipitated from zinc nitrate solution by raising the pH to ca. 8.5. The gelatinous precipitate was stirred for a further 30 min and filtered. The magnesium catalyst was precipitated from a phosphate solution using a similar method and both catalysts were prepared by calcination of the precursors using the same method as described in the previous preparations. For comparison, a fumed silica (BDH cab-o-sil) was used.

Catalysts were characterised by powder X-ray diffraction using an Enraf Nonius PSD120 diffractometer with a monochromatic Cu Kα1 source operated at 40 keV and 30 mA. Phases were identified by matching experimental patterns to the JCPDS powder diffraction file. Surface areas were determined by multi-point nitrogen adsorption at 77 K, and data were treated in accordance with the BET method.

3.2. Catalyst testing

Catalyst performance was monitored in a $\frac{1}{2}$ in. OD stainless steel plug flow microreactor operated at atmospheric pressure. Studies were performed using a methane/oxygen/helium flow of 23/2/5 ml min^{-1} and a catalyst bed volume of 0.25 cm^3, resulting in a GHSV = 7200 h^{-1}. Catalysts were pelleted to a 0.6–1.0 mm uniform particle size range and analysis was carried out on-line using gas chromatography with Porapak Q and Molsieve 5A columns in a series bypass configuration with thermal conductivity and flame ionisation detectors. The conversion was calculated on the basis of reaction products. Under the conditions used in this study, the only reaction product was CO_2 and carbon balanced were $100 \pm 2\%$ in all cases.

3.3. Theoretical

The atomic co-ordinates of β-Ga_2O_3 were taken from an experimental determination deposited at the United Kingdom Chemical Database Service [12,13]. β-Ga_2O_3 has the C2/m space group (a = 12.230 Å, b = 3.040 Å, c = 5.800 Å, β = 103.7°) with Ga^{3+} occurring in both octahedral and tetrahedral environments. In earlier work, we have used atomistic potentials with formal charges to establish that only the (0 1 0) and (0 0 1) surfaces can give rise to non-polar surfaces by simple termination of the bulk structure [14]. The (0 1 0) surface is formed from stoichiometric layers and in simpler oxides, and this is known to lead to very little surface re-structuring on optimisation of the atomic positions in the surface [15]. Optimisation under the atomistic potential model, however, lead to a rumpling of the surface with the anions moving out of the surface plane. Having reduced the number of surfaces to study, we are currently applying periodic density functional theory (DFT) to the stable surfaces, initially for comparison with the atomistic potential results, but also to enable the creation of defects and the adsorption of reactants to be studied.

We employ the Cambridge Serial Total Energy Package (CASTEP [16]) code with the generalised gradient approximation functionals due to Perdew and Wang [17] and implemented in CASTEP by White and Bird [18]. The core regions of ions was represented using ultrasoft pseudo-potentials [19]; for O^{2-}, the core was taken to be the $1s^2$ shell and for Ga^{3+}, the pseudo-potential represented orbitals up to 3p so that 4s and 3d levels were explicitly included in the plane wave representation of the valence electron band structure.

4. Results and discussion

4.1. Methane oxidation studies

The catalysts prepared in this study and the results of powder XRD and surface area measurements are summarised in Table 2.

Table 2
Results of BET surface area and phases identified by powder X-ray diffraction

Catalyst	Surface area ($m^2\,g^{-1}$)	Phase
Ga_2O_3	60	β-Ga_2O_3
1%Zn/Ga_2O_3	16	β-Ga_2O_3
1%Mg/Ga_2O_3	96	β-Ga_2O_3
ZnO	4	ZnO
$Mg_3(PO_4)_2$	3	$Mg_2P_2O_7$
SiO_2	276	Amorphous

Table 3
Methane oxidation rates at 444°C normalised for the effect of surface area

Catalyst	Rate ($mol\,s^{-1}\,m^{-2}$)
β-Ga_2O_3	7.18×10^{15}
Zn/β-Ga_2O_3	2.30×10^{16}
Mg/β-Ga_2O_3	3.24×10^{15}
ZnO	1.04×10^{16}
$Mg_2P_2O_7$	2.71×10^{16}
SiO_2	0

The surface areas of the catalysts were distributed over a relatively wide range. The precipitated magnesium and zinc catalysts were relatively low, whilst the gallium catalyst had a surface area of $60\,m^2\,g^{-1}$. The Ga_2O_3 doped with magnesium showed an increase in surface area relative to the undoped system, whilst doping with zinc reduced the surface area. Powder X-ray diffraction of the catalysts prepared from precipitated gallium nitrate and the doped counterparts containing magnesium and zinc revealed that the bulk phase was β-Ga_2O_3. The identified phases for the precipitated zinc and magnesium catalysts were ZnO and $Mg_2P_2O_7$, respectively. The fumed silica was amorphous and the surface area was much greater than the other catalysts at $276\,m^2\,g^{-1}$.

The activation of methane has been studied by methane oxidation. The results for all the catalysts tested are shown in Fig. 1. The reaction products observed were mainly carbon dioxide with trace quantities of carbon monoxide (1–2%). No other products, such as methanol, formaldehyde or ethane were detected above the limits of analytical sensitivity.

Comparison with a relative inert packing of fumed SiO_2 showed that all the catalysts were more active. Although the SiO_2 may have some residual surface activity, it provides a comparison to gauge the contribution from homogeneous gas phase reactions. The β-Ga_2O_3 catalyst and β-Ga_2O_3 doped with magnesium and zinc showed broadly similar activity. In contrast, the activity for the methane oxidation by precipitated zinc and magnesium catalysts was lower.

The data presented in Fig. 1 is representative of the catalyst formulations and is, therefore, normalised in terms of catalyst volume. To compensate for the effect of varying surface area, reaction rates have been normalised per unit area. A comparison of the normalised rates is shown in Table 3.

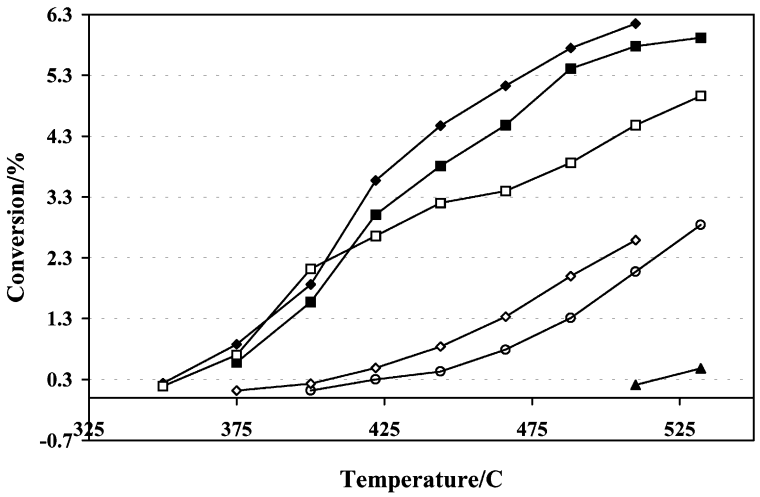

Fig. 1. Comparison of methane oxidation activity: (◆) β-Ga_2O_3; (■) Zn/β-Ga_2O_3; (□) Mg/β-Ga_2O_3; (○) ZnO; (◇) $Mg_2P_2O_7$; (▲) SiO_2.

Comparison of the gallium oxide systems in terms of surface area normalised reaction rates showed that the Zn/β-Ga_2O_3 catalyst was the most active. It is, therefore, evident that doping β-Ga_2O_3 with zinc promotes the activity for methane combustion, whilst doping with magnesium has the opposite effect and suppresses the activity. The normalised reaction rate for ZnO was less than half the rate of the Zn/β-Ga_2O_3 system, indicating that a synergistic effect for methane activation is developed when low levels of zinc are added to β-Ga_2O_3. The nature of this synergy is not clear at this early stage, but the replacement of Ga^{3+} by Zn^{2+} in the β-Ga_2O_3 lattice is a mechanism to increase the defect concentration. The molecular modelling studies are ultimately targeted to probe the type of defects created by doping and their influence on catalyst activity.

The most active surface area normalised catalyst was $Mg_2P_2O_7$. However, it was apparent that doping β-Ga_2O_3 had a detrimental effect on activity when compared to β-Ga_2O_3. The data presented in Table 2 indicated that the addition of magnesium may have an important structural promotional effect as the surface area of the doped system was considerably higher than β-Ga_2O_3. Nevertheless, the activity of $Mg_2P_2O_7$ is significant and studies are on to probe methane activation over this and related phosphate systems. The effect of doping in this study is in contrast to previous results [14]; however, the methods of catalyst preparation were different in the previous study. In the present study, all catalysts were prepared by the same precipitation method.

The activation energies for the various catalysts were calculated from the Arrhenius equation applied to the data obtained at low conversion (Table 4). The majority of activation energies were similar. Doping β-Ga_2O_3 with zinc did not significantly alter the activation energy. Doping with magnesium increased the activation energy by over 40 kJ mol^{-1} and is consistent with the lower rate observed for the Mg/β-Ga_2O_3 catalyst.

Table 4
Activation energies for methane oxidation[a]

Catalyst	Activation energy (kJ mol^{-1})
β-Ga_2O_3	123
Zn/β-Ga_2O_3	132
Mg/β-Ga_2O_3	166
ZnO	124
$Mg_2(PO_4)_2$	112

[a] Errors ± 8 kJ mol^{-1}.

4.2. Theoretical studies

4.2.1. Bulk structure of β-Ga_2O_3

Initial calculations on the bulk structure were used to converge the system with respect to plane wave cut-off energy (360 eV) and number of *k*-points (3 × 3 × 2, a total of six unique points). Geometry optimisation of the unit cell led to a small (1%) expansion in the cell vectors and this expanded structure was used to fix the surface vectors for subsequent surface calculations. The density of states calculated for the bulk structure gave an estimated band gap in the material of 2.7 eV. Although this considerably underestimates the experimental estimate from spectroscopic studies (4.9 eV [20]), it is in line with other density functional studies of solid state insulators where the structural properties are well produced despite this deficiency.

4.2.2. Surface simulation

The (0 1 0) surface was generated in the simulation studies by extension of the *b*-vector to introduce a 10 Å vacuum gap between the simulation slab and its images in the *b*-direction. The structure was re-optimised as before, but with only a single *k*-point used in the direction perpendicular to the surface. In this initial work, we compare a 3-atomic layer slab with a 5-layer. The central layer of each was held fixed to represent the bulk structure with the resulting surfaces shown in Figs. 2 and 3. For the 3-layer slab, considerable puckering of the surface occurred with the cations relaxing toward the centre of the slab between 0.14 and 0.18 Å with the surface anions showing little vertical movement. For the 5-layer case, the re-ordering is more pronounced with cation movements into the slab 0.23 Å and anion movements out of the slab by between 0.08 and 0.15 Å. A further optimisation of the 5-layer slab without a constrained central layer showed almost identical results. The additional freedom for relaxation of the second atomic layer also leads to lower calculated surface energy for the 5-layer case as shown in Table 5.

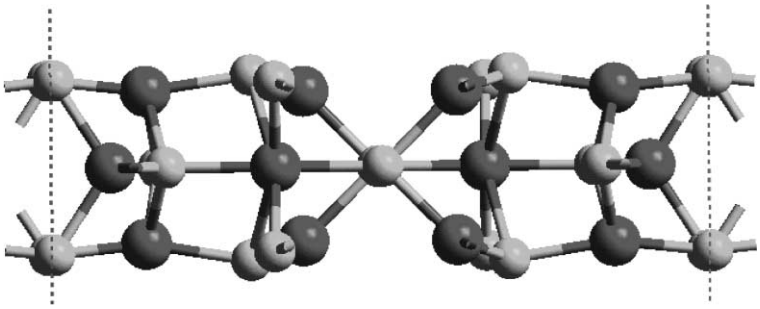

Fig. 2. 3-Layer slab model of the (0 1 0) surface of β-Ga_2O_3 after CASTEP minimisation. O: dark grey spheres, Ga: light grey spheres.

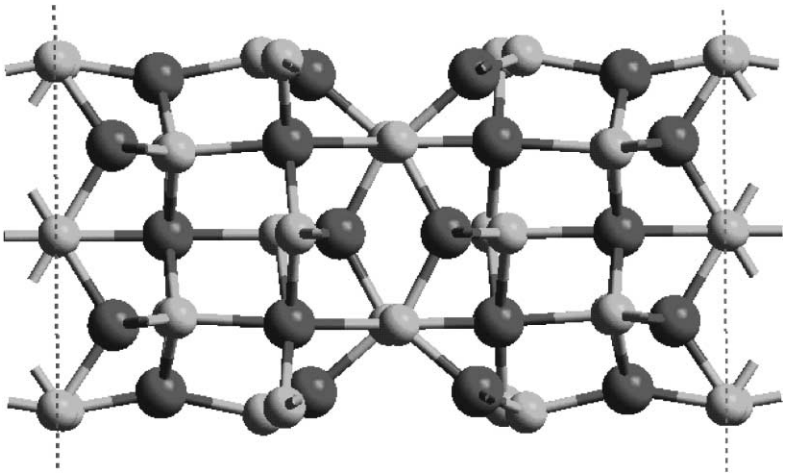

Fig. 3. 5-Layer slab model of the (0 1 0) surface of β-Ga_2O_3 after CASTEP minimisation. O: dark grey spheres, Ga: light grey spheres.

Table 5
Calculated surface energies for simulation slabs[a]

Number of slab layers	Calculated surface energy ($J\,m^{-1}$)	
	Bulk termination	Relaxed surface
3	2.20	1.70
5	2.24	1.48

[a] Surface energy is defined as the energy per unit surface area required to create the total slab surface in the simulation cell.

5. Conclusions

Experimental studies have shown that doping β-Ga_2O_3 with low levels of zinc promotes the activity for methane oxidation and it is proposed that this is due to an increase in the defect concentration of the catalyst. Conversely, the addition of magnesium suppressed the activity, but $Mg_2P_2O_7$ demonstrated significant activity for methane activation.

The periodic density functional calculations have confirmed the atomistic potential results which suggested that the (0 1 0) surface will undergo considerable restructuring compared to the simple bulk termination. The atomic relaxations result in cation movements toward the bulk and anion movements away from the surface. This, coupled with the larger ionic radius of the anion suggests that the simple defect free surface will favour adsorbates which can strongly interact with the anionic centres. We are currently extending our calculations to include defects by removing pairs of anions to investigate the structure of the partially reduced surface.

References

[1] J.H. Lunsford, T. Ito, Nature 314 (1985) 721.
[2] G.J. Hutchings, M.S. Scurrell, J.R. Woodhouse, Chem. Soc. Rev. 18 (1989) 251.
[3] G.J. Hutchings, M.S. Scurrell, Direct Methane Conversion by Oxidative Processes, Fundamental and Engineering Aspects, Van Nostrand Reinhold, New York, 1992, p. 200.
[4] G.J. Hutchings, M.S. Scurrell, J.R. Woodhouse, J. Chem. Soc., Chem. Commun. (1988) 253.
[5] D.A. Dowden, C.R. Schnell, G.T. Walker, in: Proceedings of the Fourth International Congress on Catalysis, Moscow, 1968, Paper 62, p. 201.
[6] K. Otsuka, M. Hatano, J. Catal. 108 (1987) 252.
[7] J.E. Lyons, P.E. Ellis Jr., V.A. Durante, Stud. Surf. Sci. Catal. 67 (1990) 99.
[8] S.H. Taylor, J.S.J. Hargreaves, G.J. Hutchings, R.W. Joyner, Catal. Today 42 (1998) 217.
[9] G.J. Hutchings, S.H. Taylor, Catal. Today 49 (1999) 105.
[10] J.D. Burrington, C.T. Kartisch, R.K. Grasselli, J. Catal. 87 (1984) 363.
[11] M. Guisnet, N.S. Gnep, F. Alario, Appl. Catal. A 89 (1992) 1.
[12] D.A. Fletcher, R.F. McMeeking, D. Parkin, J. Chem. Inf. Comput. Sci. 36 (1996) 746.
[13] S. Geller, J. Chem. Phys. 33 (1960) 676.
[14] C.A. Cooper, C.R. Hammond, G.J. Hutchings, S.H. Taylor, D.J. Willock, K. Tabata, Stud. Surf. Sci. Catal. 136 (2001) 319.
[15] G.W. Watson, E.T. Kelsey, N.H. de Leeuw, D.J. Harris, S.C. Parker, J. Chem. Soc., Faraday Trans. 92 (3) (1996) 433.
[16] CASTEP 4.2 Academic Version, licensed under the UKCP-MSI Agreement, 1999; Rev. Mod. Phys. 64 (1992) 1045.
[17] J.P. Perdew, Y. Wang, Phys. Rev. B 46 (1992) 6671.
[18] J.A. White, D.M. Bird, Phys. Rev. B 50 (1994) 4954.
[19] D. Vanderbilt, Phys. Rev. B 41 (1990) 7892.
[20] L. Binnet, D. Gourier, J. Phys. Chem. Solids 59 (1998) 1241.